Advanced Industrial and Engineering Polymer Research 6 (2023) 203–213

Contents lists available at ScienceDirect

Advanced Industrial and Engineering Polymer Research

journal homepage: http://www.keaipublishing.com/aiepr

# Polypropylene (PP) nanocomposites with transition metal (MgCoAl, MgNiAl, MgCuAl, MgZnAl) layered double hydroxides (t-LDHs): Flammability, thermal and mechanical analysis

Sajid Naseem [a, b, *], Sven Wießner [a, b], Ines Kühnert [a], Frederick J.W.J. Labuschagné [c], Andreas Leuteritz [a]

[a] Leibniz-Institut für Polymerforschung Dresden e.V., Hohe Straße 6, 01069 Dresden, Germany
[b] Institute of Materials Science, Technische Universität Dresden, 01062 Dresden, Germany
[c] Department of Chemical Engineering, University of Pretoria, Lynwood Road, Pretoria, South Africa

ARTICLE INFO

*Article history:*
Received 30 September 2022
Received in revised form
20 December 2022
Accepted 31 January 2023

*Keywords:*
Polypropylene (PP) nanocomposite
Layered double hydroxide (LDH)
Ternary metal (t-LDH) based nanocomposite
Thermal
Flammability and mechanical properties of PP nanocomposite

ABSTRACT

Over the last few years, transition metal based LDHs are drawing more and more attention. This is especially true for tri-metal LDHs due to their wide range of applications. This research work highlights four types of tri-metal layered double hydroxide (t-LDH) that were synthesized and used in polypropylene (PP) nanocomposites. The effect and interaction of cobalt (Co), nickel (Ni), copper (Cu) and zinc (Zn) containing MgAl LDHs in PP nanocomposite were prepared and tested. These t-LDHs (MgCoAl, MgNiAl, MgCuAl, MgZnAl) were synthesized using the urea hydrolysis method. The t-LDH/PP nanocomposites were prepared using melt mixing in a small-scale compounder. Structural and morphological analysis of t-LDH and their PP nanocomposites were done using XRD spectroscopy and SEM. The thermal behaviour of the nanocomposites was studied using DSC and TGA. Rheological analysis was done using a rheometer, flammability was analysed using limiting oxygen index (LOI) and UL94 testing. Mechanical properties were compared by a UTM and Charpy impact test. The thermal stability, flame retardancy and mechanical strength are increased with the addition of these t-LDHs. MgCuAl/PP nanocomposites showed superior thermal and mechanical properties as compared to MgAl/PP, MgCoAl/PP, MgNiAl/PP, MgZnAl/PP nanocomposites. In comparison to pure PP with the addition of only 5 wt.% of MgCuAl-LDH the degradation temperature was 43 °C higher.



## 1. Introduction

Layered double hydroxides (LDHs) are interesting materials for various applications because of their multifunctional nature, tunable properties and tunable structure. LDHs are known as anionic clays with the formula of $[M_1^{2+}{}_xMx^{3+}(OH)_2]^{x+}.[(A^{n-})_{x/n}.yH_2O]^x$ where $M^{2+}$, $M^{3+}$ and $A^{n-}$ are divalent metal cations, trivalent metal cations and interlayer anions respectively [1–3]. Allmann and Taylor first discussed the structure and properties of LDHs [4,5]. LDHs are useful and being used from many years as a multifunctional material, because of possible changes in structure either in layers or in combinations of cations, easy synthesis methods with multiple sources and procedures [3]. There are various possibilities of changes in the structure such as in metallic cations, compositions, combinations of metals or replacement in the interlayer anions [6,7]. Combinations of different cations are also interesting possibilities in the change of LDH structure such as bi-metallic combinations, tri-metallic or multi-metallic combinations of LDHs. The application and use of these LDHs mainly depend on the metals involved in the structure and the method used for the synthesis of these LDHs [8–14]. There are different techniques available to synthesise such LDHs with a variety of metallic composition such as urea hydrolysis and co-precipitation, hydrothermal synthesis and ion exchange methods. The most commonly studied layered double hydroxides are bi-metallic combinations of LDHs [2,6,7,15]. LDHs were used in a range of applications in

* Corresponding author. Leibniz-Institut für Polymerforschung Dresden e.V., Hohe Straße 6, 01069 Dresden, Germany.
*E-mail addresses:* naseem@ipfdd.de (S. Naseem), wiessner@ipfdd.de (S. Wießner), kuehnert@ipfdd.de (I. Kühnert), johan.labuschagne@up.ac.za (F.J.W.J. Labuschagné), leuteritz@ipfdd.de (A. Leuteritz).

https://doi.org/10.1016/j.aiepr.2023.01.007

different sectors such as in the pharmaceutical industry [16], in biomedical applications [17–20], in wastewater treatments [21], as UV–Vis absorption materials [11,22–24], in a photovoltaic cell and solar cells [24], in supercapacitors [25], in sensors [26], as acid scavengers [27], as antioxidants [28], as a catalyst [29,30], as flame retardant for polymers [31–35] and as stabilizers for polymers [36,37]. LDHs can be used in different aspects such as coolant and producing diluent for flammable gas [38], as a flame retardant supporting resistance to ignition in polymers [39] or LDHs can provide an alternate way of combustion by a slower rate of flame spread and can reduce the quantity of smoke [16,39]. Jiang et al. (2016) used organically modified ZnAl LDHs with zirconium 2-(2-(2-aminoethylamino)ethylamino)ethylphosphonate (ZrP) in PP to enhance flame retardancy of PP [40]. Qiu et al. (2018) studied the thermal and flame-retardant properties of PP nanocomposites with organically modified MgAl LDHs. The best flame retardant performance was achieved in case of PP/stearic LDH(24h) with 20 wt.% loading of LDHs [41].

Bi-metallic combinations of LDHs were studied more commonly and MgAl is one of the most widely studied combinations of bi-metallic LDHs [42–46]. There are various possibilities to create multifunctionality in MgAl LDH structure and the most common is the organic modification of MgAl LDHs. Such organic modifications can increase the miscibility of LDH with polymers. The other option to create multifunctionality is to introduce a third metal in the MgAl structure. These third metal substitutions are less commonly studied and very few studies are available on their interaction with polymers. Mostly organic modified MgAl LDH was used in polymers previously and synthesized using the co-precipitation method. There are some studies available such as Zhu et al. (2010) synthesized MgCuAl-LDH with various anion intercalations and thermal stability of MgCuAl/PVC was observed. The thermal stability of PVC was enhanced with the addition of MgCuAl LDH in PVC [47,48]. Wang et al. (2015) synthesized combinations of Mg, Al and Zn LDH via the co-precipitation method and organically modified them with SDBS. The tensile strength of these LDHs/polypropylene (PP) composites was slightly lower than PP [49]. Nagendra et al. (2017) synthesized Zn–Al, Co–Al, and CoZnAl LDH via the co-precipitation method and used it in PP, and studied the effect on PP [50]. Gomez et al. (2019) synthesized MgZnAl via co-precipitation with intercalation of nitrate and *p*-aminobenzoate. They used these LDH in polyethylene (PE) and it can be observed that these modified MgZnAl LDH can be a possible filler to avoid PE from UV degradation [51]. These previously studied tri-metal LDHs were synthesized using the co-precipitation method and most of them were organically modified to use in polymers to improve mixing and processing. Naseem et al. (2021) synthesized MgFeAl LDH via urea hydrolysis and used it in polypropylene (PP). A decrease in mechanical properties and increased catalytic degradation were observed in MgFeAl/PP nanocomposites [52]. Method of synthesis (urea hydrolysis, co-precipitation) also affects structural growth and eventually the properties of such transition metal LDHs [53,54].

In most of the previous research work on LDHs/PP composites, researchers used bi-metallic LDHs either unmodified or organically modified to analyse the properties of PP composites [55–59]. There is a wide range of transition metals available which can be substituted in MgAl LDHs and then can be used in polymers to analyse and compare the properties. In this research work, transition metals (Co, Ni, Cu, Zn) substituted MgAl-LDHs (t-LDHs) were used to prepare PP nanocomposites. The t-LDHs were synthesized using the urea hydrolysis method and nanocomposites of t-LDH/PP were prepared using the melt mixing method. All the LDHs and their PP nanocomposites were characterized and analysed in detail using XRD, SEM, flammability analysis, thermal, rheological and mechanical analysis. The focus of this research work is to investigate and compare the effect of these t-LDHs (MgCoAl, MgNiAl, MgCuAl, MgZnAl) on various properties of PP nanocomposites.

## 2. Materials and methods

$Mg(NO_3)_2 \cdot 6H_2O$, $Al(NO_3)_3 \cdot 9H_2O$, $Co(NO_3)_2 \cdot 6H_2O$, $Ni(NO_3)_2 \cdot 6H_2O$, $Cu(NO_3)_2 \cdot 3H_2O$, $Zn(NO_3)_2 \cdot 6H_2O$ were purchased from ABCR. Urea ($CO(NH_2)_2$) was bought from Sigma Aldrich. Chemically pure (CP) or analytical grade (AR) reactants were used for all experiments without further treatment. Distilled water was used for the preparation of salt solutions and all the processes. Polypropylene (PP) (HD120MO) was bought from Borealis A/S Denmark. PP functionalized with maleic anhydride (MA) (SCONA TPPP 2112 FA), obtained from BYK additives & instrument Germany.

### 2.1. Synthesis of tri-metal layered double hydroxides (t-LDHs): MgAl, MgCoAl, MgNiAl, MgCuAl and MgZnAl LDHs

MgAl, MgCoAl, MgNiAl, MgCuAl and MgZnAl-LDH were synthesized via urea hydrolysis as explained in the literature [6,15]. A molar ratio of 2:1 ($M^{II+}$:$M^{III+}$) was used for the synthesis of these t-LDHs. The transition metals (M = Co, Ni, Cu, Zn) were substituted as follows: $M/(Mg + M) = 0.1$ for Co, Ni, Cu and Zn (all on a molar basis). $Co(NO_3)_2 \cdot 6H_2O$, $Ni(NO_3)_2 \cdot 6H_2O$, $Cu(NO_3)_2 \cdot 3H_2O$, $Zn(NO_3)_2 \cdot 6H_2O$, $Mg(NO_3)_2 \cdot 6H_2O$ and $Al(NO_3)_2 \cdot 9H_2O$ salts were dissolved in distilled water in the desired amount. A round bottom flask was used for salt solutions and the temperature was given 100 °C for 48 h. At the finish of the reaction, the slurries were cooled down to room temperature for all types of t-LDHs and then these slurries were filtered and washed with distilled water. The filtered t-LDHs were dried in the heating oven for 24 h at 70 °C. The schematic illustrations for the synthesis of MgAl, MgCoAl, MgNiAl, MgCuAl, and MgZnAl-LDHs (t-LDHs) using urea hydrolysis are shown in Fig. 1.

### 2.2. Preparation of t-LDH/PP nanocomposites

All these t-LDH/PP nanocomposites were prepared in a small-scale compounder (Thermo Scientific-Germany, Process 11) with 5 wt.% of MgAl, MgCoAl, MgNiAl, MgCuAl, and MgZnAl LDHs as described in Fig. 2 and Table 1. The temperature used for preparing these LDH/PP nanocomposites was 190 °C and the screw rotation speed was set to 100 rpm. Samples for mechanical properties (tensile strength, impact strength) and flammability testing (LOI, UL94) were synthesized via injection molding process using a Dr. Boy 22 A HV (Dr. Boy Machine Incorporation, Germany). The details of LDH/PP samples and their respective ratios of t-LDH used in PP are shown in Table 1.

### 2.3. Characterization methods

X-ray diffraction measurements were performed on a Panalytical X'Pert PRO X-ray diffractometer in θ–θ configuration, equipped with a Fe filtered Co-Kα radiation (1.789 Å) and with an X'Celerator detector and variable divergence and fixed receiving slits. The data was collected in the angular range $5° \leq 2\theta \leq 80°$ with a step size of 0.008° 2θ and a 13 s scan step time. Scanning electron microscopy (SEM) images of t-LDHs were taken with a Zeiss Ultra Plus. TGA measurement was performed with a heating rate of 10 °C/min using a TGA Q5000 from TA instruments in an inert nitrogen atmosphere and air atmosphere. The temperature range of 25 °C–800 °C was used for TGA analysis. Differential scanning calorimeter (DSC) analysis was done using DSC Q2000 from TA instruments. Three cycles of heating-cooling-heating with a heating/cooling rate of 10 °C/min and a sample size of about 5 mg were

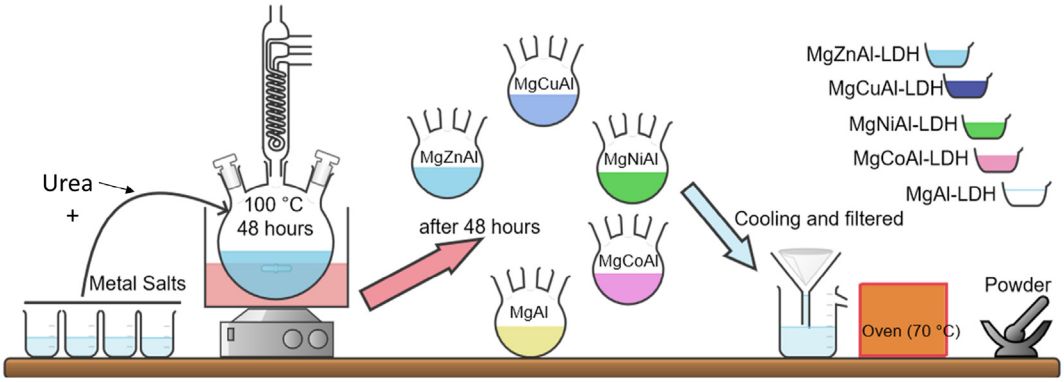


**Fig. 1.** Schematic representation of the synthesis of transition metal-based (t-LDHs), (MgAl, MgCoAl, MgNiAl, MgCuAl, MgZnAl) synthesized using urea hydrolysis.

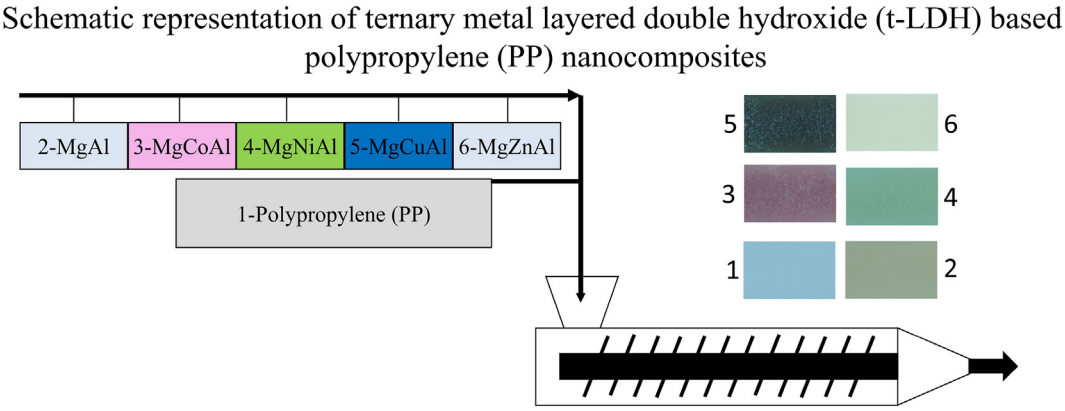


**Fig. 2.** Schematic representation of transition metal-based t-LDH/PP nanocomposites using a small-scale compounder. Different colours of t-LDH/PP nanocomposites such as 1 (PP), 2 (MgAl/PP), 3 (MgCoAl/PP), 4 (MgNiAl/PP), 5 (MgCuAl) and 6 (MgZnAl/PP) depending on the colour of t-LDHs shown.

**Table 1**
Sample details of transition metal-based t-LDHs/PP nanocomposites. Each t-LDHs have a different colour depending on the substitution of transition metals and these colours can be observed in t-LDH/PP samples also.

| Sr. No. | LDHs | Amount (wt. %) | PP (wt. %) |
|---|---|---|---|
| 1 | - | 0 | 100 |
| 2 | MgAl | 5 | 95 |
| 3 | MgCoAl | 5 | 95 |
| 4 | MgNiAl | 5 | 95 |
| 5 | MgCuAl | 5 | 95 |
| 6 | MgZnAl | 5 | 95 |

used. The thermograms of the second heating cycle were analysed for the study of the melting behavior of the samples. The flammability analysis was done using limiting oxygen index (LOI) measurements on an oxygen index meter (FTT, UK) (ASTM D2863-19). The burning rate was determined via UL94 V and UL94 HB testing using the method described previously [60]. UL94 HB (horizontal burning) is used to determine the burning in mm/min of the testing material. Rheological analysis of t-LDH/PP nanocomposites was done in oscillatory shear using a strain-controlled rheometer (ARES, Rheometrics Scientific, USA). The analysis was done over a frequency range of 0.1–100 rad/s at 180 °C and 5% strain. Tensile properties of t-LDH/PP nanocomposites were analysed according to DIN EN ISO 527-2/1BA/50 with a Zwick 1456 (model 1456, Z010, Ulm Germany) (length: 82 mm, width: 10 mm, thickness: 2 mm) with a crosshead speed of 50 mm $min^{-1}$. The Charpy impact strength of t-LDH/PP nanocomposites was measured using the standard ISO 179/1eU by PSW 15J. The results of t-LDH/PP nanocomposites were averaged over five measurements for each sample for the tensile, Charpy impact and flammability testing. All the t-LDHs/PP nanocomposites prepared for flammability and mechanical testing were injection molded under identical conditions at 180 °C. Scanning electron microscopy (SEM) images of fractured specimens of t-LDH/PP nanocomposites were taken with a Zeiss Ultra Plus.

## 3. Results and discussion

### 3.1. XRD and SEM analysis of transition metal (t-LDH)

X-ray diffraction (XRD) spectroscopy and scanning electron microscopy (SEM) was used to analyse the structure and morphology of synthesized t-LDHs. The XRD graphs of t-LDH (MgAl, MgCoAl, MgNiAl, MgCuAl and MgZnAl) are shown in Fig. 3(a–e) respectively with their SEM images. The peaks of XRD patterns of MgAl and transition metal substituted (Co, Ni, Cu, Zn) MgAl LDHs are narrow and sharp which represents that there are no contaminations in these synthesized t-LDHs. High-intensity peeks at (003), (006), (009) and (110) are observed in the XRD pattern, indicating a well-ordered structure of t-LDHs [31,61–63]. Higher substitution of transition metal in MgAl-LDH could increase the amorphous phase in the t-LDHs and can decrease the growth of layered structure in LDHs which ultimately can reduce the

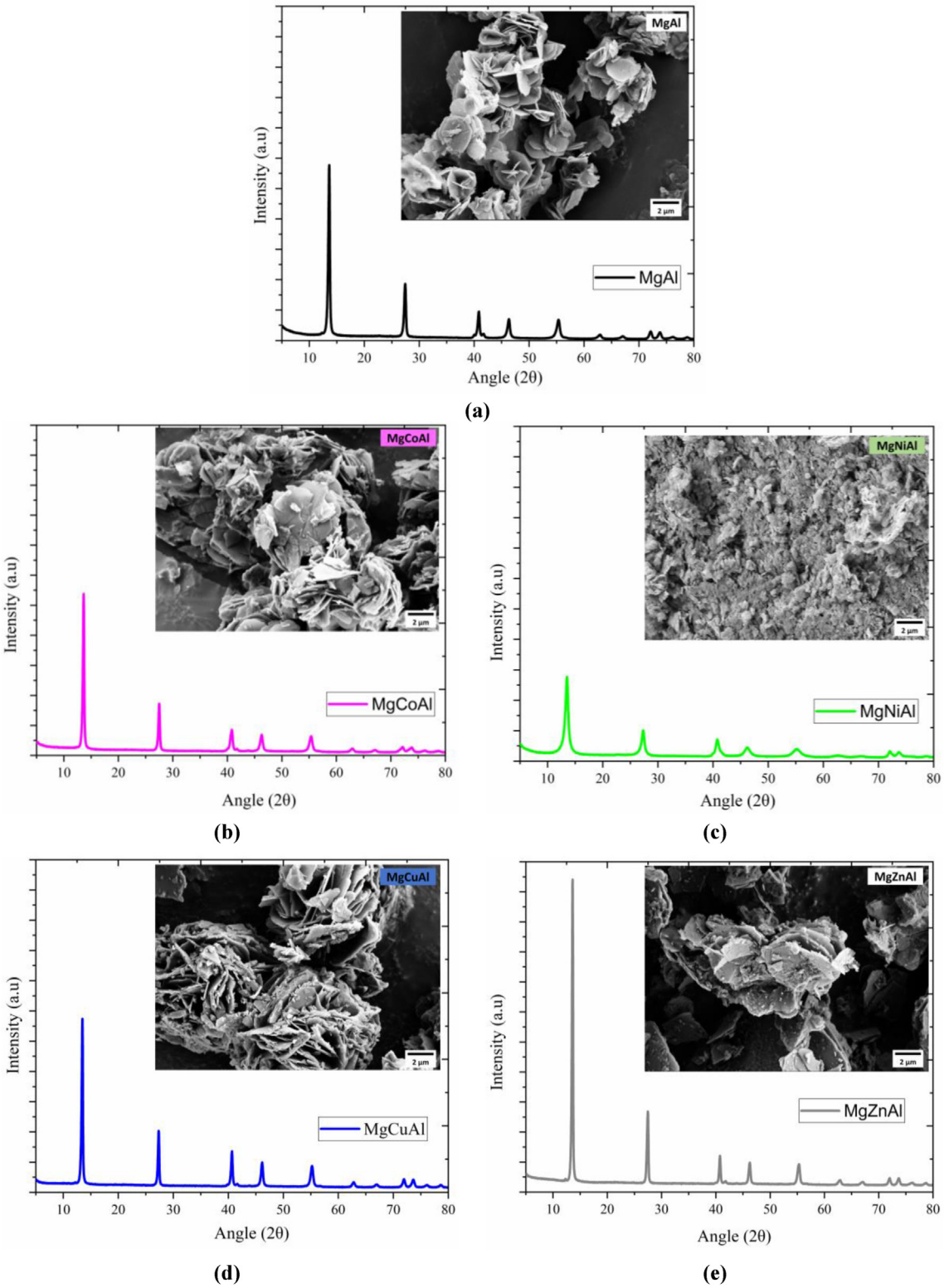


**Fig. 3.** X-ray diffraction (XRD) and SEM images of (a) MgAl (b) MgCoAl (c) MgNiAl (d) MgCuAl (e) MgZnAl t-LDH. These t-LDHs show the characteristic structure and morphology of LDHs synthesized via the urea hydrolysis.

crystallinity of LDHs structures [53,64]. MgAl, MgCoAl, MgNiAl, MgCuAl, and MgZnAl showed hexagonal platelets structure which is the characteristic of synthesized LDHs which are synthesized using urea hydrolysis. The platelets are relatively larger and thin except in the case of MgNiAl. Synthesis of t-LDHs via the urea hydrolysis method usually gives the large and well-ordered structure of t-LDHs. The larger platelet size of such LDHs is the result of the hydrolysis of the urea used during the reaction process [15]. The

**Table 2**
Colour parameters (L*, a*, b*) and opacity values of pure PP and t-LDHs/PP nanocomposites measured by spectrophotometer with samples images.

| Sr. No. | t-LDH/PP nanocomposites | Color parameters (L*, a*, b*) | Opacity | Sample images |
|---|---|---|---|---|
| 1 | PP | 65.3, 0.81, 6.8 | 22.5 | |
| 2 | MgAl/PP | 51.8, 2.14, 13.6 | 48.8 | |
| 3 | MgCoAl/PP | 39.6, 8.16, 3.4 | 90.6 | |
| 4 | MgNiAl/PP | 48.2, -2.5, 14.2 | 47.4 | |
| 5 | MgCuAl/PP | 27.4, -0.54, 0.95 | 94.2 | |
| 6 | MgZnAl/PP | 49.2, 1.4, 10.6 | 56.5 | |

morphologies of these t-LDH are also different from each other as can be seen in SEM images because of the substitution of transition metals (Co, Ni, Cu and Zn). This change in morphology and layered structure can also affect the thermal and mechanical properties of t-LDHs/PP nanocomposites as different transition metals can have different interactions and dispersion in PP during melt processing.

### *3.2. Colour parameters (L*, a*, b*) and opacity measurements of t-LDHs/PP nanocomposites*

The opacity values and colour parameters (L*, a*, b*) were analysed and measured using a spectrophotometer and the values are written in Table 2, which shows that compounded pure PP has some scattering due to the semi-crystalline nature of PP. The colour of PP was almost transparent and the colour of MgAl/PP nanocomposites is turbid because of the MgAl-LDH colour. The colours of each t-LDHs/PP nanocomposite are different from each other because of the different colours of transition metals based LDHs. The different colour pictures of t-LDH/PP nanocomposites are also shown in Table 2 which are depending on the colour of t-LDHs. The colour of MgCoAl/PP, MgNiAl/PP, MgCuAl/PP and MgZnAl/PP nanocomposites are light red-brown, light green, light blue and white colour respectively because of the colour of t-LDH as shown in Table 2. The values of "L" parameters show the trend of PP > MgAl > MgZnl > MgNiAl > MgCoAl > MgCuAl composites as can be observed in Table 2 and Fig. 4. This is showing that the impact of colour can also be observed in t-LDHs/PP nanocomposites. The value of "L" parameter is lowest and opacity is highest in the case of MgCuAl/PP nanocomposites which is 27.37 and 94.21 respectively. and the lowest value of opacity is in the case of PP which is 22.53.

The opacity of t-LDH-based PP nanocomposites is higher as compared to pure PP. The addition of MgAl, MgZnAl, and MgCoAl was lighter in colour as observed from spectrophotometer values. The addition of MgCuAl showed a darker colour and the darkest colour was due to the addition of MgCuAl in PP. The addition of each t-LDH to PP gives different values of L*a*b and opacity as shown in Table 2 and Fig. 4. The opacity value increased as the dispersion of t-LDH particles increased because of the scattering phenomena of t-LDH [52]. MgCuAl/PP showed the highest (94.2) opacity values and pure PP showed the lowest (22.5) and this can be related to the higher dispersion of MgCuAl LDH in PP. Better dispersion of MgCuAl can also be related to thermal and mechanical properties in comparison to other t-LDH/PP nanocomposites.

### *3.3. Limiting oxygen index (LOI), UL94 and burning testing of t-LDHs/PP nanocomposites*

Table 3 shows the values of the limiting oxygen index (LOI) for t-LDH/PP nanocomposites. The values of LOI provide initial information on flame retardancy for polymer nanocomposites [52]. PP nanocomposites based on t-LDH show different values of LOI because of the different natures of t-LDH/PP nanocomposites. LOI

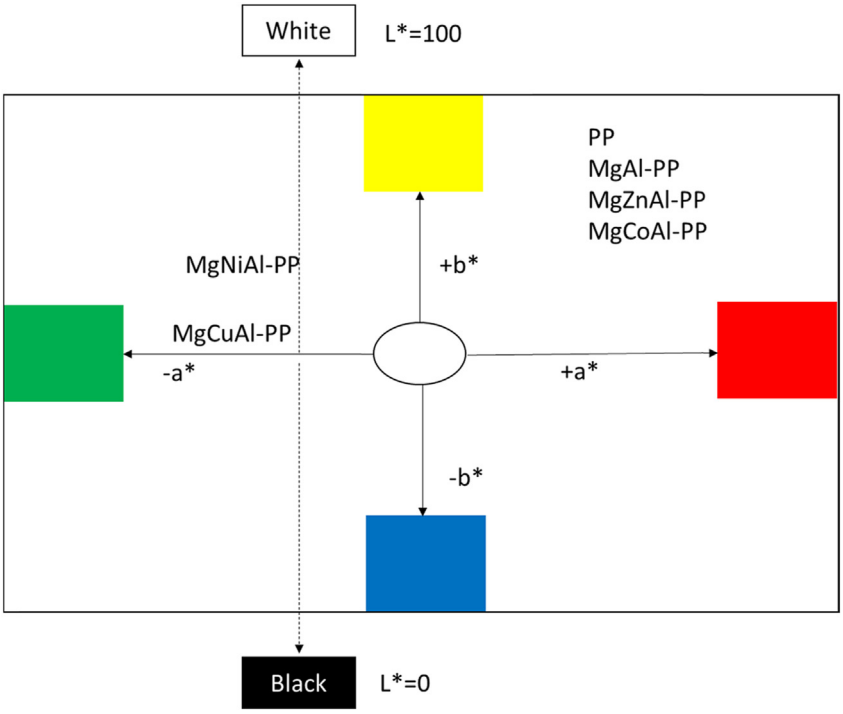


**Fig. 4.** Colour parameters measured using spectrophotometer showing colour range and opacity of t-LDHs/PP nanocomposites and pure PP, MgCuAl/PP showing the highest opacity and lowest L value.

**Table 3**
Limiting Oxygen Index (LOI) of various transition metal based t-LDHs/PP nanocomposites.

| Sr. No. | t-LDH/PP nanocomposites | Limiting Oxygen Index (LOI) |
|---|---|---|
| 1 | PP | 20 ± 0.08 |
| 2 | MgAl/PP | 20.8 ± 0.11 |
| 3 | MgCoAl/PP | 21.2 ± 0.16 |
| 4 | MgNiAl/PP | 21.4 ± 0.16 |
| 5 | MgCuAl/PP | 22.2 ± 0.13 |
| 6 | MgZnAl/PP | 23.2 ± 0.18 |

value for pure PP is 20 and with the addition of MgAl, MgCuAl, MgNiAl, MgCoAl, and MgZnAl-LDH the values are 20.8, 21.2, 21.4, 22.2, 23.2 respectively. With the addition of t-LDHs in PP the burning behavior of PP changed as compared to pure PP. Pure PP burns like a candle and burns continuously with continuous melt drips until the whole sample was consumed. The burning of t-LDH/PP nanocomposites was different as these samples showed three regions on the burning surface such as skin layers consisting of char and then melting layers supported by a solid surface. As the loading level of all t-LDH was only 5 wt.% in all the cases so the formation of char was not higher. Previously researchers used up to 20 wt.% of MgAl-LDH in polyethylene (PE) and increase in LOI was from 18 to 22 while in case of 2.5, and 5 wt.% there was no increase in LOI [43]. The substitution of transition metal in MgAl LDH provides an increase in LOI values of t-LDH/PP nanocomposites and this can be interlinked with the change in the structure of t-LDH due to substitution of transition metals leading to a change in LOI values of PP nanocomposites.

The images of burned t-LDHs/PP nanocomposites are shown in Fig. 5. The values of the burning rate of each t-LDHs/PP nanocomposites are shown in Table 4. UL94 test was done with vertical (UL94V) and horizontal (UL94 HB) burning tests. No rating of these tests was observed in these burning analyses. But still, the useful information and basic difference in these t-LDH/PP were observed and shown in Table 4 in terms of burning rate.

The burning rate decreased accordingly (MgAl > MgCoAl > MgNiAl > MgCuAl > MgZnAl) as shown in Table 4. Substitution of 3rd transition metal changes the structure as discussed previously and also shows the decrease in the burning rate at this low loading level (5 wt.%). Previously studied MgAl/PE composites and clay/PP nanocomposites also showed no UL94 ratings at these low loading levels [43,65].

### 3.4. Thermogravimetric analysis (TGA) of t-LDHs/PP nanocomposites

The influence of the transition metal based t-LDHs on the thermal behavior of PP nanocomposites was studied using TGA. The decomposition in nitrogen and in air for t-LDH/PP nanocomposites

**Table 4**
The burning rate of different transition metal based t-LDHs/PP nanocomposites.

| Sr. No. | t-LDH/PP nanocomposites | Burning Rate (mm/min) |
|---|---|---|
| 1 | PP | 14.37 ± 0.16 |
| 2 | MgAl/PP | 14.9 ± 0.15 |
| 3 | MgCoAl/PP | 14.04 ± 0.19 |
| 4 | MgNiAl/PP | 12.94 ± 0.10 |
| 5 | MgCuAl/PP | 11.8 ± 0.10 |
| 6 | MgZnAl/PP | 11.65 ± 0.12 |

was done and the results are shown in Fig. 6(a–c) and Fig. 1S. The substitution of these transition metals (Co, Ni, Cu, Zn) in MgAl LDH structure results in a difference in the thermal behavior of PP nanocomposites as can be observed in Fig. 6 (a, b). The TGA curves for the t-LDHs/PP nanocomposites are very similar to that of the pure PP with a difference in decomposition rate. The addition of MgCuAl-LDH in PP shows the largest increase in thermal stability of PP nanocomposites as can be seen in Fig. 6(a–c) and Table 5. As the t-LDHs were added to PP nanocomposites the thermal stability enhances depending on the type and nature of t-LDHs.

The maximum weight loss temperature ($T_{max}$) of different PP nanocomposite systems is shown in Table 5. The peaks shift towards higher temperatures with the addition of t-LDH in PP as can be seen in Fig. 6. Unexpectedly, the system containing no transition metal shows the earliest degradation maximum, and the system containing Cu has the largest shift. The maximum weight loss temperature for pure PP is 300 °C. Maximum weight loss temperatures for MgAl, MgCoAl, MgNiAl, MgCuAl and MgZnAl are 325, 318, 326, 343 and 330 °C respectively. It can be observed that MgCuAl provides an increase of 43 °C in maximum weight loss temperature. Further, MgCuAl also showed better dispersion as compared to all other t-LDHs and this better mixing could also be the reason for the higher thermal stability of PP nanocomposites. The substitution of transition metals in MgAl LDH can change the thermal stability of t-LDHs and eventually the thermal stability of PP nanocomposites, and here copper (Cu) is giving the highest increase as can be observed in Fig. 6(a–c) and Table 5. To better understand the thermal stability, 50% weight loss temperature is also shown in Table 5 which is also highest in the case of MgCuAl LDH as compared to other LDHs. It can be easily said from TGA analysis that MgCuAl/PP nanocomposites show better thermal stability as compared to all other t-LDH/PP nanocomposites and this can be interlinked with colour parameters values in which MgCuAl/PP showed the highest opacity values.

### 3.5. Differential scanning calorimetry (DSC) analysis of t-LDHs/PP nanocomposites

Fig. 7 (a, b) are showing the DSC analysis of t-LDHs/PP nanocomposites. The addition of the t-LDHs (MgAl, MgCoAl, MgNiAl,

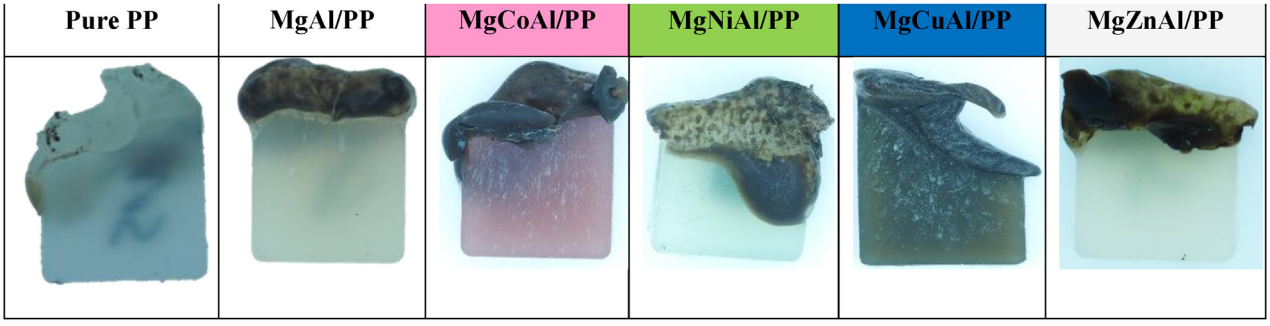


**Fig. 5.** Images of the samples after flammability analysis of transition metal based t-LDHs/PP nanocomposites.

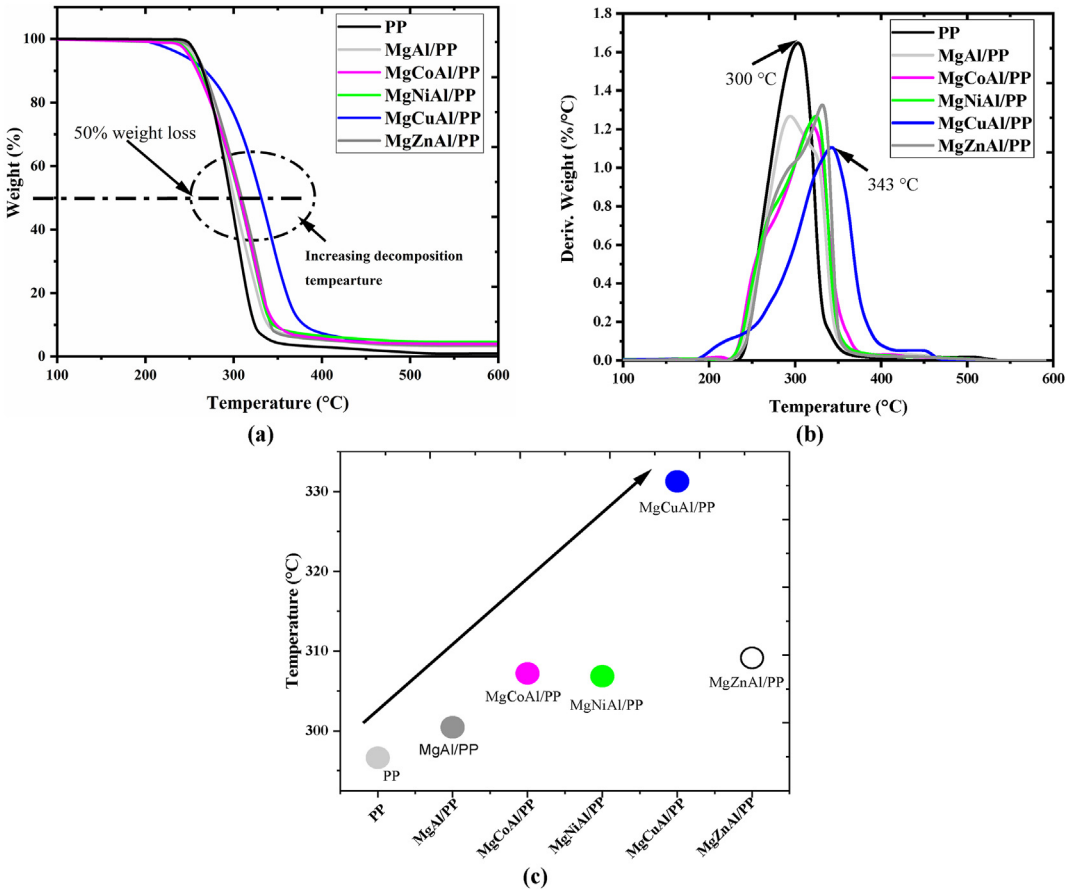


**Fig. 6.** Thermogravimetric analysis (TGA) of transition metal based t-LDHs/PP nanocomposites in nitrogen environment (a) TGA (b) Derivative TGA (c) influence of t-LDHs on decomposition temperature at 50% weight loss ($T_{0.5}$) indicating Copper (Cu) substituted MgAl showing the highest thermal stability for PP nanocomposites as compared to other t-LDHs.

MgCuAl, MgZnAl) in PP resulted in higher melt crystallization peak temperature as compared to pure PP. This higher melt crystallization peak temperature indicates a higher nucleation activity which is interlinked with higher dispersion in PP [52]. The structures of transition metal based LDHs are different from each other as observed in this study, resulting in different crystallization temperatures of PP nanocomposites. The substitution of transition metals (Co, Ni, Cu, Zn) into MgAl-LDH changed the structure of these t-LDH such as *d*(003), c parameters, and crystallite sizes [6,7]. The change in the charge structures of these t-LDHs due to the substitution of transition metals could lead to a change in the nucleation and crystallization of PP nanocomposites. The estimated crystallite size of MgCuAl was higher than MgCoAl, MgNiAl, MgZnAl [6]. The better match of structural parameters between MgCuAl-LDHs and PP could lead to higher nucleation/crystallization in MgCuAl/PP nanocomposites [66]. It was also observed previously that the addition of LDH and MMT could lead to an increase in crystallization temperature [66]. The small increase in interlayer spacing could already increase the crystallization temperature ($T_c$) as shown previously in the case of MgFeAl-LDH/PP nanocomposites [52]. Nagendra et al. (2015) studied the effect of the particle size of LDH on the crystallization of PP. They observed better nucleation ability of PP in the presence of sonicated LDHs. This can be interlinked with the higher surface area and high dispersion of LDH in PP [67]. Shi et al. (2010) studied the crystallinity and thermal stability of LDH based PP composites. They studied the effect of organic modification using sodium dodecyl sulfate on MgAl LDH. As the LDH added the crystallinity of PP increased and this is more prominent in the case of organo-modified LDHs. An increase in crystallinity eventually causes an increase in thermal stability and flame retardancy [68].

**Table 5**
Temperature at which maximum weight loss occurred ($T_{max}$) and temperature at which 50% weight loss occurred ($T_{0.5}$) in t-LDHs/PP nanocomposite under a nitrogen environment.

| Sr. No. | t-LDH/PP nanocomposites | $T_{max}$ (°C) | $T_{0.5}$ (°C) |
|---|---|---|---|
| 1 | PP | 300 | 296.6 |
| 2 | MgAl/PP | 325 | 300.5 |
| 3 | MgCoAl/PP | 318 | 307.2 |
| 4 | MgNiAl/PP | 326 | 306.9 |
| 5 | MgCuAl/PP | 343 | 331.3 |
| 6 | MgZnAl/PP | 330 | 309.2 |

### 3.6. Rheological analysis of t-LDHs/PP nanocomposites

The rheological analysis provides basic information about melt processability and particle dispersion of t-LDH in polypropylene (PP) [69]. The rheological properties of t-LDHs/PP nanocomposites depend on the dispersion and interaction of t-LDH in PP. Fig. 8(a, b) shows the complex viscosity and tan delta values of MgAl/PP, MgCoAl/PP, MgNiAl/PP, MgCuAl/PP, MgZnAl/PP nanocomposites and pure PP. The viscosity of PP decreased as the t-LDHs were

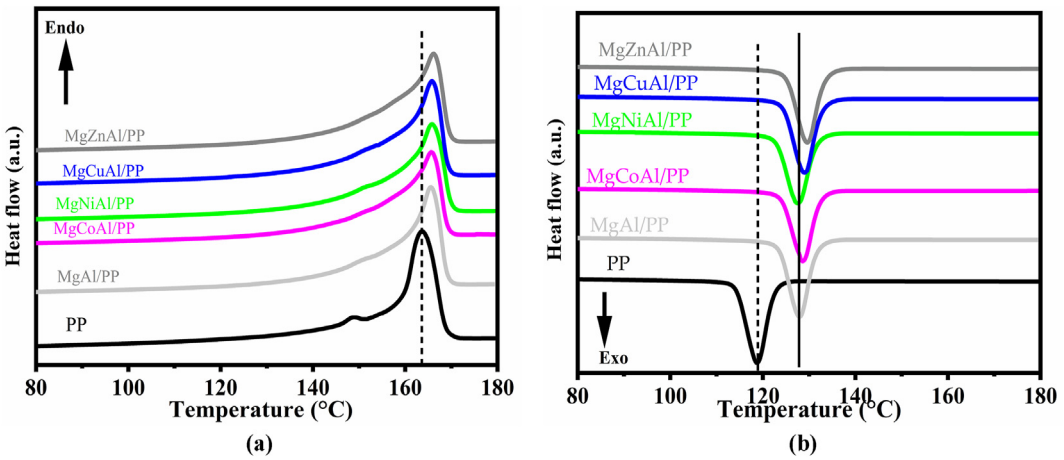


**Fig. 7.** DSC thermograms of transition metal based t-LDHs/PP nanocomposites (a) heating curve (b) cooling curve.

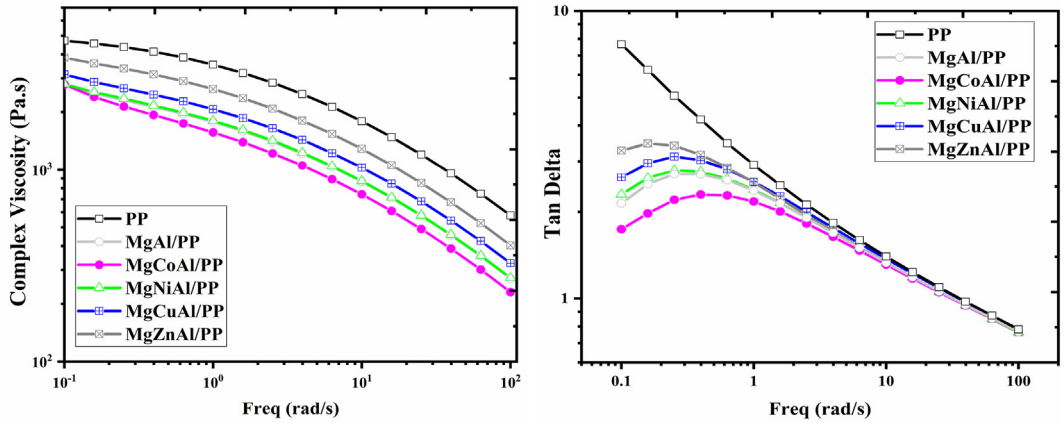


**Fig. 8.** Rheological analysis of different transition metal based t-LDHs/PP nanocomposites performed at 180 °C.

added to PP because of chain relaxations. The addition of fillers can cause a decrease in complex viscosity and this is because of an increase in free volume and dilution effect [69].

The decrease in complex viscosity is highest in the case of MgCoAl/PP nanocomposites. The addition of the transition metal as a third metal in MgAl-LDH showed a direct impact on the rheological properties of t-LDHs/PP nanocomposites and these results can be interlinked with previously discussed results. The degradation reaction could occur during melt processing and the addition of compatibilizers could also cause a decrease in the complex viscosity of different t-LDHs/PP nanocomposites. Wang et al. observed similar results when they studied polypropylene (PP)/$Mg_3Al$−tartrazine LDH- nanocomposites and observed a decrease in viscosity [69]. Wang et al. conferred that when the average particle separation distance is lesser than twice the polymer radius of gyration *Rg* then the nanofiller will interrupt polymer chain configurations and cause a reduction in the viscosity [69].

### *3.7. Mechanical properties and morphological analysis of t-LDHs/PP nanocomposites*

Table 6 is showing the mechanical properties (modulus, tensile strength and impact strength) of MgAl/PP, MgCoAl/PP, MgNiAl/PP, MgCuAl/PP and MgZnAl/PP nanocomposites. The tensile strength and impact strength are higher in the case of pure PP as compared to t-LDH/PP nanocomposites. The melt processing and compatibilizer caused degradation as discussed in the rheological section and this can also affect the tensile strength [66]. Nanocomposites of t-LDH/PP have lower values as compared to pure PP because of the degradation during melt processing and due to the compatibilizer effect. When comparing t-LDH/PP nanocomposites the Youngs modulus and tensile strength are highest in the case of MgCuAl/PP nanocomposites. It can be seen in Table 6 that the addition of MgCuAl in PP is showing the highest modulus (1783 MPa) and tensile strength (35 MPa) as compared to MgAl/PP, MgCoAl/PP, MgNiAl/PP, MgZnAl/PP.

Higher dispersion during the mixing of MgCuAl in PP as compared to other t-LDH provides higher modulus and tensile strength. The dispersion of MgCuAl in PP as compared to other t-

**Table 6**
Mechanical properties of transition metal based t-LDHs/PP nanocomposites, Young's modulus, tensile strength and impact strength.

| Sr. No. | t-LDHs/PP nanocomposites | Youngs modulus (MPa) | Tensile strength (MPa) | Charpy impact strength (kJ/m²) |
|---|---|---|---|---|
| 1 | PP | 1340±32 | 37.3±1.5 | 110±11 |
| 2 | MgAl/PP | 1710±100 | 34.3±0.8 | 55.4±4.3 |
| 3 | MgCoAl/PP | 1745±64 | 34.6±0.56 | 46.9±4.4 |
| 4 | MgNiAl/PP | 1713±95 | 34.2±0.26 | 49.1±6.1 |
| 5 | MgCuAl/PP | 1783±102 | 35.0±0.50 | 62.5±4.2 |
| 6 | MgZnAl/PP | 1767±70 | 34.8±0.28 | 79.3±3.6 |

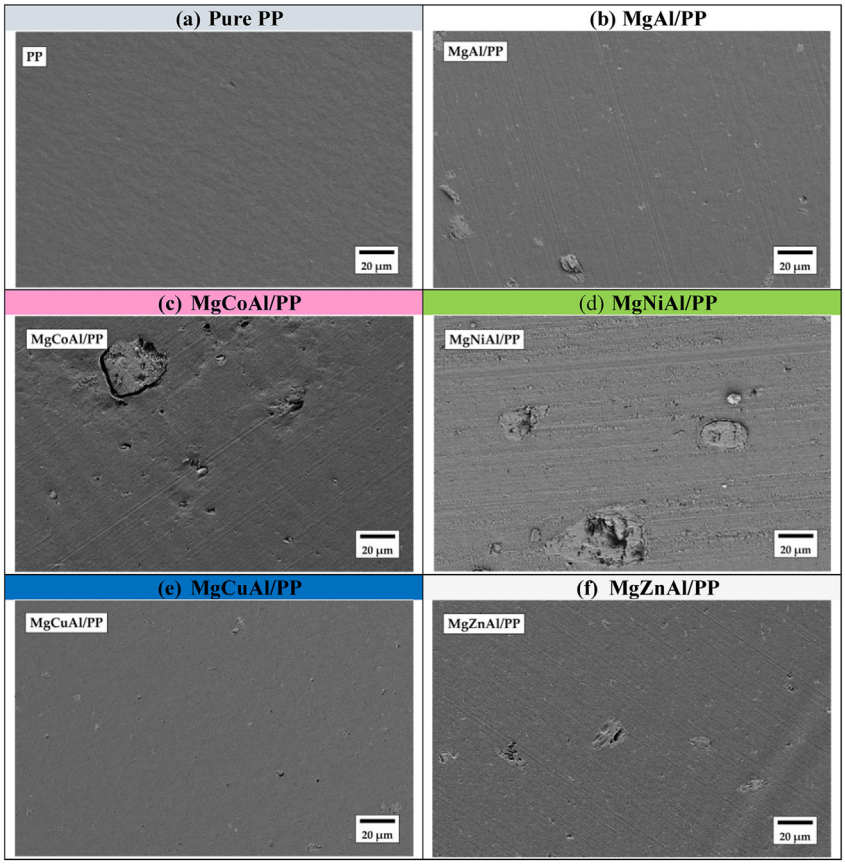


**Fig. 9.** SEM images of fractured samples of pure polypropylene (PP) and transition metal based t-LDH-PP nanocomposites (a) PP (b) MgAl/PP (c) MgCoAl/PP (d) MgNiAl/PP (e) MgCuAl/PP (f) MgZnAl/PP nanocomposites.

LDHs can also be observed in SEM images of fractured samples (Fig. 9). The mixing and intercalation of each transition metal based LDHs in PP is shown as a schematic in Fig. 10 and this scheme is designed on the bases of SEM images of fractured samples and previously discussed thermal, colour analysis, rheological and mechanical testing results.

It can be observed that MgCuAl shows no agglomerates in PP nanocomposites and the best dispersion as compared to other

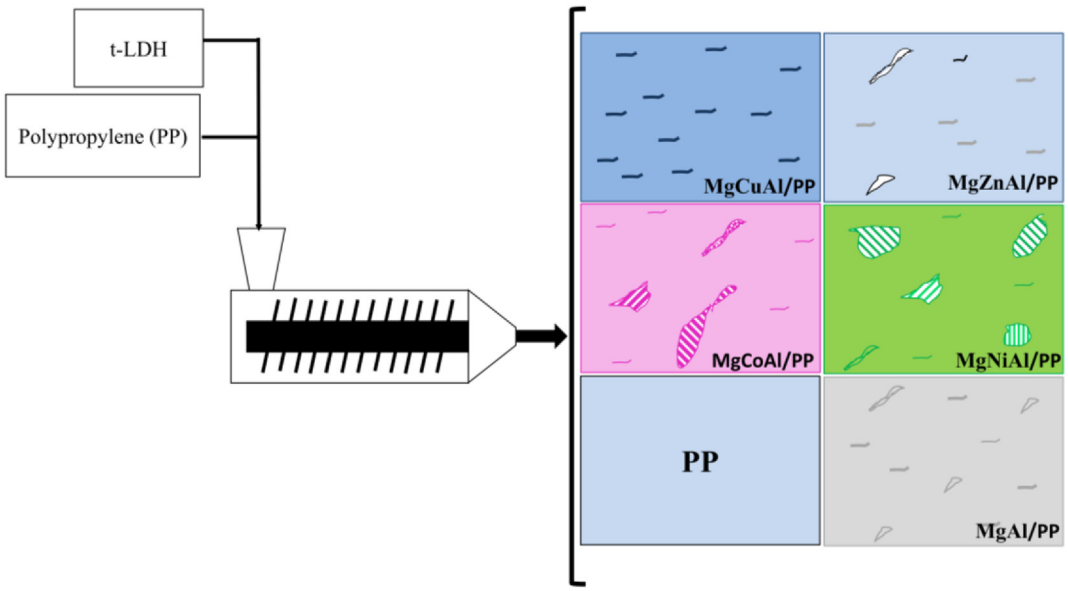


**Fig. 10.** Schematic representation of transition metal-based t-LDH/PP nanocomposites. The highest dispersion was obtained in the case of MgCuAl/PP nanocomposites as compared to other t-LDH which can be correlated to SEM images, higher thermal and mechanical properties of MgCuAl/PP nanocomposites.

t-LDH/PP nanocomposites. MgCoAl and MgNiAl LDH showed large agglomeration in PP nanocomposites and the lowest dispersion. MgAl-LDH and MgZnAl-LDH also show some agglomeration in PP nanocomposites and resulting in low mechanical properties. These mechanical properties analysis can be interlinked with previous analyses of colour parameters, flammability and thermal analysis results and it can be said that MgCuAl LDH can provide good dispersion in PP and eventually could get better thermal and mechanical properties. In the case of MgNiAl/PP and MgCoAl/PP nanocomposites, large agglomerates of LDH particles can be observed in Fig. 9 which lead to poor dispersion and eventually lead to the lowest tensile strength as compared to other t-LDH/PP nanocomposites [70,71]. Tensile strength and Young's modulus show the trend of (MgCuAl/PP > MgZnAl/PP, MgCoAl > MgNiAl/PP).

## 4. Conclusion

The effect and interaction of transition metal-based t-LDH/PP nanocomposites were analysed and compared. The substitution of transition metals (Co, Ni, Cu, Zn) in MgAl-LDH changed the layered structure, surface area, particle size and morphology of these t-LDHs. Due to the presence of different types of transition metals (Co, Ni, Cu, Zn) in MgAl-LDH, the colour parameters, flammability, thermal behavior, rheological properties, mechanical properties and interaction were different in each t-LDH/PP nanocomposites. From colour parameters, it can be observed that MgCuAl/PP nanocomposites showed the highest opacity values. DSC analysis of t-LDH/PP showed a nucleation effect due to the presence of transition metals, TGA comparison showed that MgCuAl/PP nanocomposites showed the highest thermal stability as compared to other t-LDH/PP nanocomposites. The intercalation and miscibility of MgCuAl in PP were also the highest as observed from SEM analysis of fractured samples. The degradation temperature was 43 °C higher as compared to pure PP with the addition of only 5 wt.% of MgCuAl-LDH. From the comparison of mechanical, thermal, flammability, colour, rheological and morphological analysis of t-LDH/PP nanocomposites it can be said that MgCuAl/PP showed higher miscibility, thermal and mechanical properties as compared to other t-LDHs/PP nanocomposites. A higher amount of t-LDH or organic modification can be done and analysed to compare the effect of these LDH on PP or in other polymers.

## Declaration of competing interest

The authors declare no conflict of interest.

## Acknowledgments

We thank Kerstin Arnhold for providing the TGA results on time.

## Appendix A. Supplementary data

Supplementary data to this article can be found online at https://doi.org/10.1016/j.aiepr.2023.01.007.

## References

[1] Y. Kuang, L. Zhao, S. Zhang, F. Zhang, M. Dong, S. Xu, Morphologies, preparations and applications of layered double hydroxide micro-/nanostructures, Materials 3 (2010) 5220–5235.
[2] R. Xu, Y. Xu (Eds.), Modern Inorganic Synthetic Chemistry, second ed., Elsevier, Amsterdam, 2017, pp. 493–543.
[3] S. Naseem, A. Leuteritz, U. Wagenknecht, in: S. Kenig (Ed.), Processing of Polymer Nanocomposites, Hanser, 2019, pp. 343–369.
[4] R. Allmann, The crystal structure of pyroaurite, Acta Crystallogr. B 24 (1968) 972–977.
[5] H.F.W. Taylor, Segregation and Cation-Ordering in Sjogrenite and Pyroaurite Mineralogical Magazine, 37, 1969, pp. 338–342.
[6] S. Naseem, B. Gevers, R. Boldt, F.J.W.J. Labuschagné, A. Leuteritz, Comparison of transition metal (Fe, Co, Ni, Cu, and Zn) containing tri-metal layered double hydroxides (LDHs) prepared by urea hydrolysis, RSC Adv. 9 (2019) 3030–3040.
[7] B.R. Gevers, S. Naseem, A. Leuteritz, F.J.W.J. Labuschagné, Comparison of nanostructured transition metal modified tri-metal MgMAl–LDHs (M = Fe, Zn, Cu, Ni, Co) prepared using co-precipitation, RSC Adv. 9 (2019) 28262–28275.
[8] D.-K. Cho, C.-W. Jeon, I.-K. Park, Growth and optical band gap of CdAl-layered double hydroxide thin structures on rigid substrate, J. Alloys Compd. 737 (2018) 725–730.
[9] J.J. Bravo-Suárez, E.A. Páez-Mozo, S.T. Oyama, Review of the synthesis of layered double hydroxides: a thermodynamic approach, Quím. Nova 27 (2004) 601–614.
[10] C. Forano, U. Costantino, V. Prévot, C.T. Gueho, in: F. Bergaya, G. Lagaly (Eds.), Developments in Clay Science, Elsevier, 2013, pp. 745–782, vol. 5.
[11] B.R. Gevers, S. Naseem, C.J. Sheppard, A. Leuteritz, F.J.W.J. Labuschagne, Modification of Layered Double Hydroxides Using First-Row Transition Metals for Superior UV-Vis-NIR Absorption and the Influence of the Synthesis Method Used, 2020.
[12] Z. Yu, X. Li, Y. Peng, X. Min, D. Yin, L. Shao, MgAl-layered-double-hydroxide/sepiolite composite membrane for high-performance water treatment based on layer-by-layer hierarchical architectures, Polymers 11 (2019).
[13] Z. Karami, M.R. Ganjali, M. Zarghami Dehaghani, M. Aghazadeh, M. Jouyandeh, A. Esmaeili, S. Habibzadeh, A. Mohaddespour, Inamuddin, K. Formela, J.T. Haponiuk, M.R. Saeb, Kinetics of cross-linking reaction of epoxy resin with hydroxyapatite-functionalized layered double hydroxides, Polymers 12 (2020) 1157.
[14] V. Bugatti, G. Viscusi, A. Di Bartolomeo, L. Iemmo, D.C. Zampino, V. Vittoria, G. Gorrasi, Ionic liquid as dispersing agent of LDH-carbon nanotubes into a biodegradable vinyl alcohol polymer, Polymers 12 (2020) 495.
[15] J. He, M. Wei, B. Li, Y. Kang, D.G. Evans, X. Duan, in: X. Duan, D.G. Evans (Eds.), Layered Double Hydroxides, Springer Berlin Heidelberg, Berlin, Heidelberg, 2006, pp. 89–119.
[16] F. Li, X. Duan, in: X. Duan, D.G. Evans (Eds.), Layered Double Hydroxides, Springer Berlin Heidelberg, Berlin, Heidelberg, 2006, pp. 193–223.
[17] G. Mishra, B. Dash, S. Pandey, Layered double hydroxides: a brief review from fundamentals to application as evolving biomaterials, Appl. Clay Sci. 153 (2018) 172–186.
[18] S. Bujok, J. Hodan, H. Beneš, Effects of immobilized ionic liquid on properties of biodegradable polycaprolactone/LDH nanocomposites prepared by in situ polymerization and melt-blending techniques, Nanomaterials 10 (2020) 969.
[19] E. Vasile, I.-C. Radu, B. Galateanu, M. Rapa, A. Hudita, D. Jianu, P.-O. Stanescu, H. Cioflan, C. Zaharia, Novel nanocomposites based on bacterial polyester/LDH-SDS clay for stem cells delivery in modern wound healing management, Materials 13 (2020) 4488.
[20] H. Beneš, J. Kredatusová, J. Peter, S. Livi, S. Bujok, E. Pavlova, J. Hodan, S. Abbrent, M. Konefał, P. Ecorchard, Ionic liquids as delaminating agents of layered double hydroxide during in-situ synthesis of poly (butylene adipate-co-terephthalate) nanocomposites, Nanomaterials 9 (2019) 618.
[21] O. Alagha, M.S. Manzar, M. Zubair, I. Anil, N.D. Mu'azu, A. Qureshi, Comparative adsorptive removal of phosphate and nitrate from wastewater using biochar-MgAl LDH nanocomposites: coexisting anions effect and mechanistic studies, Nanomaterials 10 (2020) 336.
[22] J. Jiménez Reinosa, P. Leret, C.M. Álvarez-Docio, A. del Campo, J.F. Fernández, Enhancement of UV absorption behavior in ZnO–$TiO_2$ composites, Bol. Soc. Espanola Ceram. Vidr. 55 (2016) 55–62.
[23] S. Naseem, S.P. Lonkar, A. Leuteritz, Study of modified LDHs as UV protecting materials for polypropylene (PP), AIP Conf. Proc. 2055 (2019), 050002.
[24] S. Naseem, B.R. Gevers, F.J.W.J. Labuschagné, A. Leuteritz, Preparation of photoactive transition-metal layered double hydroxides (LDH) to replace dye-sensitized materials in solar cells, Materials 13 (2020).
[25] G. Yang, T. Takei, S. Yanagida, N. Kumada, Enhanced supercapacitor performance based on CoAl layered double hydroxide-polyaniline hybrid electrodes manufactured using hydrothermal-electrodeposition technology, Molecules 24 (2019) 976.
[26] C. Zhang, X. Liang, Y. Lu, H. Li, X. Xu, Performance of CuAl-LDH/Gr nanocomposite-based electrochemical sensor with regard to trace glyphosate detection in water, Sensors 20 (2020) 4146.
[27] Y.-J. Lin, D.-Q. Li, D.G. Evans, X. Duan, Modulating effect of Mg–Al–$CO_3$ layered double hydroxides on the thermal stability of PVC resin, Polym. Degrad. Stabil. 88 (2005) 286–293.
[28] S.P. Lonkar, A. Leuteritz, G. Heinrich, Antioxidant intercalated layered double hydroxides: a new multifunctional nanofiller for polymers, RSC Adv. 3 (2013) 1495–1501.
[29] G. Fan, F. Li, D.G. Evans, X. Duan, Catalytic applications of layered double hydroxides: recent advances and perspectives, Chem. Soc. Rev. 43 (2014) 7040–7066.
[30] S. Naseem, B. Gevers, F.J.W.J. Labuschagné, A. Leuteritz, Catalytic degradation study of iron (Fe) containing LDH-PP composites, AIP Conf. Proc. 2289 (2020), 020041.
[31] Y. Gao, J. Wu, Q. Wang, C.A. Wilkie, D. O'Hare, Flame retardant polymer/layered double hydroxide nanocomposites, J. Mater. Chem. 2 (2014) 10996–11016.
[32] Y. Gao, Q. Wang, W. Lin, Ammonium polyphosphate intercalated layered double hydroxide and zinc borate as highly efficient flame retardant nanofillers for polypropylene, Polymers 10 (2018).

[33] B.-n. Wang, M.-y. Chen, B.-j. Yang, Modification and compounding of CaMgAl-layered double hydroxides and their application in the flame retardance of acrylonitrile-butadiene-styrene resin, Polymers 11 (2019) 1623.
[34] Y. Gao, Q. Wang, W. Lin, Ammonium polyphosphate intercalated layered double hydroxide and zinc borate as highly efficient flame retardant nano-fillers for polypropylene, Polymers 10 (2018) 1114.
[35] M.J. Mochane, S.I. Magagula, J.S. Sefadi, E.R. Sadiku, T.C. Mokhena, Morphology, thermal stability, and flammability properties of polymer-layered double hydroxide (LDH) nanocomposites: a review, Crystals 10 (2020) 612.
[36] B. Kutlu, A. Leuteritz, L. Häußler, U. Oertel, G. Heinrich, Stabilization of polypropylene using dye modified layered double hydroxides, Polym. Degrad. Stabil. 102 (2014) 9–14.
[37] S. Naseem, S.P. Lonkar, A. Leuteritz, F.J.W.J. Labuschagné, Different transition metal combinations of LDH systems and their organic modifications as UV protecting materials for polypropylene (PP), RSC Adv. 8 (2018) 29789–29796.
[38] G. Camino, A. Maffezzoli, M. Braglia, M. De Lazzaro, M. Zammarano, Effect of hydroxides and hydroxycarbonate structure on fire retardant effectiveness and mechanical properties in ethylene-vinyl acetate copolymer, Polym. Degrad. Stabil. 74 (2001) 457–464.
[39] X. Wang, Q. Zhang, Effect of hydrotalcite on the thermal stability, mechanical properties, rheology and flame retardance of poly(vinyl chloride), Polym. Int. 53 (2004) 698–707.
[40] T. Jiang, C. Liu, L. Liu, J. Hong, M. Dong, X. Deng, Synergistic flame retardant properties of a layered double hydroxide in combination with zirconium phosphonate in polypropylene, RSC Adv. 6 (2016) 91720–91727.
[41] L. Qiu, Y. Gao, C. Zhang, Q. Yan, D. O'Hare, Q. Wang, Synthesis of highly efficient flame retardant polypropylene nanocomposites with surfactant intercalated layered double hydroxides, Dalton Trans. 47 (2018) 2965–2975.
[42] F.R. Costa, M. Saphiannikova, U. Wagenknecht, G. Heinrich, Wax Crystal Control · Nanocomposites · Stimuli-Responsive Polymers, Springer Berlin Heidelberg, Berlin, Heidelberg, 2008, pp. 101–168.
[43] F.R. Costa, U. Wagenknecht, G. Heinrich, LDPE/Mg–Al layered double hydroxide nanocomposite: thermal and flammability properties, Polym. Degrad. Stabil. 92 (2007) 1813–1823.
[44] F.R. Costa, M. Abdel-Goad, U. Wagenknecht, G. Heinrich, Nanocomposites based on polyethylene and Mg–Al layered double hydroxide. I. Synthesis and characterization, Polymer 46 (2005) 4447–4453.
[45] R. Quispe-Dominguez, S. Naseem, A. Leuteritz, I. Kuehnert, Synthesis and characterization of MgAl-DBS LDH/PLA composite by sonication-assisted masterbatch (SAM) melt mixing method, RSC Adv. 9 (2019) 658–667.
[46] Z. Karami, S.M.R. Paran, P. Vijayan P, M.R. Ganjali, M. Jouyandeh, A. Esmaeili, S. Habibzadeh, F.J. Stadler, M.R. Saeb, A comparative study on cure kinetics of layered double hydroxide (LDH)/Epoxy nanocomposites, J. Compos. Sci. 4 (2020) 111.
[47] H. Zhu, W. Wang, T. Liu, Effects of copper-containing layered double hydroxide on thermal and smoke behavior of poly(vinyl chloride), J. Appl. Polym. Sci. 122 (2011) 273–281.
[48] F.J.W.J. Labuschagne, D.M. Molefe, W.W. Focke, I. van der Westhuizen, H.C. Wright, M.D. Royeppen, Heat stabilising flexible PVC with layered double hydroxide derivatives, Polym. Degrad. Stabil. 113 (2015) 46–54.
[49] X. Wang, Y. Spörer, A. Leuteritz, I. Kuehnert, U. Wagenknecht, G. Heinrich, D.-Y. Wang, Comparative study of the synergistic effect of binary and ternary LDH with intumescent flame retardant on the properties of polypropylene composites, RSC Adv. 5 (2015) 78979–78985.
[50] B. Nagendra, C.V.S. Rosely, A. Leuteritz, U. Reuter, E.B. Gowd, Polypropylene/layered double hydroxide nanocomposites: influence of ldh intralayer metal constituents on the properties of polypropylene, ACS Omega 2 (2017) 20–31.
[51] N.A.G. Gomez, F. Wypych, Nanocomposites of polyethylene and ternary (Mg + Zn/Al) layered double hydroxide modified with an organic UV absorber, J. Polym. Res. 26 (2019) 203.
[52] S. Naseem, S. Wießner, I. Kühnert, A. Leuteritz, Layered double hydroxide (MgFeAl-LDH)-Based polypropylene (PP) nanocomposite: mechanical properties and thermal degradation, Polymers 13 (2021) 3452.
[53] K. Parida, M. Satpathy, L. Mohapatra, Incorporation of $Fe^{3+}$ into Mg/Al layered double hydroxide framework: effects on textural properties and photocatalytic activity for $H_2$ generation, J. Mater. Chem. 22 (2012) 7350–7357.
[54] H.T. Kang, K. Lv, S.L. Yuan, Synthesis, characterization, and $SO_2$ removal capacity of MnMgAlFe mixed oxides derived from hydrotalcite-like compounds, Appl. Clay Sci. 72 (2013) 184–190.
[55] Y. Feng, D. Li, Y. Wang, D.G. Evans, X. Duan, Synthesis and characterization of a UV absorbent-intercalated Zn–Al layered double hydroxide, Polym. Degrad. Stabil. 91 (2006) 789–794.
[56] H. Chai, Y. Lin, D.G. Evans, D. Li, Synthesis and UV absorption properties of 2-Naphthylamine-1,5-disulfonic acid intercalated Zn–Al layered double hydroxides, Ind. Eng. Chem. Res. 47 (2008) 2855–2860.
[57] R. Charifou, F. Gouanvé, R. Fulchiron, E. Espuche, Polypropylene/layered double hydroxide nanocomposites: synergistic effect of designed filler modification and compatibilizing agent on the morphology, thermal, and mechanical properties, J. Polym. Sci. B Polym. Phys. 53 (2015) 782–794.
[58] G. Wang, S. Xu, C. Xia, D. Yan, Y. Lin, M. Wei, Fabrication of host-guest UV-blocking materials by intercalation of fluorescent anions into layered double hydroxides, RSC Adv. 5 (2015) 23708–23714.
[59] Y. Peng, W. Wang, J. Cao, Y. Huang, Synthesis of 5-sulfosalicylic acid-intercalated layered double hydroxide and its effects on wood flour/polypropylene composites during accelerated UV weathering, J. Appl. Polym. Sci. 134 (2017), 44597.
[60] F.R. Costa, U. Wagenknecht, G. Heinrich, LDPE/Mg-Al layered double hydroxide nanocomposite: thermal and flammability properties, Polym. Degrad. Stabil. 92 (2007) 1813–1823.
[61] Y.-M. Zheng, N. Li, W.-D. Zhang, Preparation of nanostructured microspheres of Zn–Mg–Al layered double hydroxides with high adsorption property, Colloids Surf. A Physicochem. Eng. Asp. 415 (2012) 195–201.
[62] L.H. Chagas, G.S.G. De Carvalho, W.R. Do Carmo, R.A.S. San Gil, S.S.X. Chiaro, A.A. Leitão, R. Diniz, L.A. De Sena, C.A. Achete, MgCoAl and NiCoAl LDHs synthesized by the hydrothermal urea hydrolysis method: structural characterization and thermal decomposition, Mater. Res. Bull. 64 (2015) 207–215.
[63] N. Iyi, T. Sasaki, Decarbonation of MgAl-LDHs (layered double hydroxides) using acetate–buffer/NaCl mixed solution, J. Colloid Interface Sci. 322 (2008) 237–245.
[64] L. Chmielarz, P. Kuśtrowski, A. Rafalska-Łasocha, R. Dziembaj, Influence of Cu, Co and Ni cations incorporated in brucite-type layers on thermal behaviour of hydrotalcites and reducibility of the derived mixed oxide systems, Thermochim. Acta 395 (2002) 225–236.
[65] U. Wagenknecht, B. Kretzschmar, G. Reinhardt, Investigations of fire retardant properties of polypropylene-clay-nanocomposites, Macromol. Symp. vol. 194 (2003) 207–212.
[66] M. Ardanuy, J.I. Velasco, V. Realinho, D. Arencón, A.B. Martínez, Non-isothermal crystallization kinetics and activity of filler in polypropylene/Mg-Al layered double hydroxide nanocomposites, Thermochim. Acta 479 (2008) 45–52.
[67] B. Nagendra, K. Mohan, E.B. Gowd, Polypropylene/layered double hydroxide (LDH) nanocomposites: influence of LDH particle size on the crystallization behavior of polypropylene, ACS Appl. Mater. Interfaces 7 (2015) 12399–12410.
[68] Y. Shi, F. Chen, J. Yang, M. Zhong, Crystallinity and thermal stability of LDH/polypropylene nanocomposites, Appl. Clay Sci. 50 (2010) 87–91.
[69] Q. Wang, J. Wu, Y. Gao, Z. Zhang, J. Wang, X. Zhang, X. Yan, A. Umar, Z. Guo, D. O'Hare, Polypropylene/$Mg_3Al$–tartrazine LDH nanocomposites with enhanced thermal stability, UV absorption, and rheological properties, RSC Adv. 3 (2013) 26017–26024.
[70] T. Wu, Y. Tong, F. Qiu, D. Yuan, G.z. Zhang, J.p. Qu, Morphology, rheology property, and crystallization behavior of PLLA/OMMT nanocomposites prepared by an innovative eccentric rotor extruder, Polym. Adv. Technol. (2017) 1–11.
[71] Y. Zheng, Y. Chen, Preparation of polypropylene/Mg–Al layered double hydroxides nanocomposites through wet pan-milling: non-isothermal crystallization behaviour, R. Soc. Open Sci. 5 (2018).